AD-A182 339 INTEGRATED OPTICAL INFORMATION PROCESSING(U) CALIFORNIA 1/1
INST OF TECH PASADENA DEPT OF ELECTRICAL ENGINEERING
D PSALTIS ET AL. 21 MAY 87 AFOSR-TR-87-0850
UNCLASSIFIED AFOSR-84-0339 F/G 20/6 NL

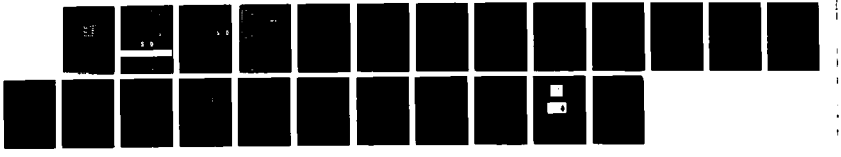

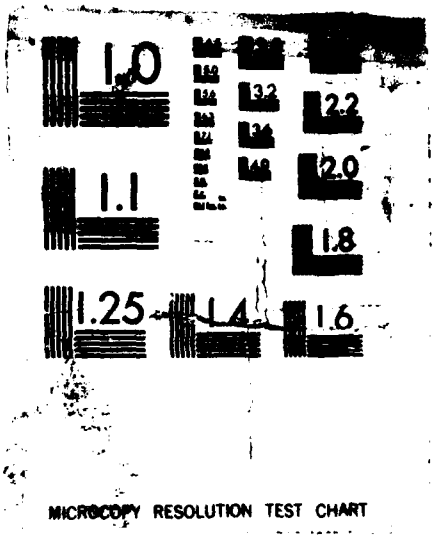
1.0
1.1
1.25
1.4
1.6
2.2
2.0
1.8
MICROCOPY RESOLUTION TEST CHART

INTEGRATED OPTICAL INFORMATION PROCESSING

Demetri Psaltis and David Brady

CALIFORNIA INSTITUTE OF TECHNOLOGY

(2)

Final Report

INTEGRATED OPTICAL INFORMATION PROCESSING

Demetri Psaltis and David Brady

Grant AFOSR-84-0339

Submitted to:
Air Force Office of Scientific Research
Bolling Air Force Base
Washington, DC

Principal Investigator

Demetri Psaltis
Department of Electrical Engineering
California Institute of Technology
Pasadena,CA, 91125

SECURITY CLASSIFICATION OF THIS PAGE

REPORT DOCUMENTATION PAGE

1a. REPORT SECURITY CLASSIFICATION: Unclassified	1b. RESTRICTIVE MARKINGS
2a. SECURITY CLASSIFICATION AUTHORITY	3. DISTRIBUTION/AVAILABILITY OF REPORT: Unlimited
2b. DECLASSIFICATION/DOWNGRADING SCHEDULE	
4. PERFORMING ORGANIZATION REPORT NUMBER(S): AFOSR-85-0339	5. MONITORING ORGANIZATION REPORT NUMBER(S): AFOSR-TR- 87-0850
6a. NAME OF PERFORMING ORGANIZATION: California Institute of Technology; 6b. OFFICE SYMBOL (If applicable)	7a. NAME OF MONITORING ORGANIZATION: AFOSR
6c. ADDRESS (City, State and ZIP Code): Department of Electrical Engineering, Mail Stop 116-81, Pasadena, CA, 91125	7b. ADDRESS (City, State and ZIP Code): Bldg 410, Bolling AFB, DC 20332
8a. NAME OF FUNDING/SPONSORING ORGANIZATION: Same as 7a; 8b. OFFICE SYMBOL (If applicable): NE	9. PROCUREMENT INSTRUMENT IDENTIFICATION NUMBER: AFOSR-85-0339
8c. ADDRESS (City, State and ZIP Code): Same as 7b	10. SOURCE OF FUNDING NOS. — PROGRAM ELEMENT NO.: 61102; PROJECT NO.: 2305; TASK NO.: B4; WORK UNIT NO.:
11. TITLE (Include Security Classification): Integrated Optical Information Processing	
12. PERSONAL AUTHOR(S): Demetri Psaltis	
13a. TYPE OF REPORT: Final; 13b. TIME COVERED: FROM 85Sep30 TO 86Dec31	14. DATE OF REPORT (Yr., Mo., Day): 5/21/1987; 15. PAGE COUNT: 19
16. SUPPLEMENTARY NOTATION	

17. COSATI CODES			18. SUBJECT TERMS (Continue on reverse if necessary and identify by block number)
FIELD	GROUP	SUB. GR.	

19. ABSTRACT (Continue on reverse if necessary and identify by block number)

The goal of this project is the development of techniques that will permit integrated optical devices to be used in inherently nonplanar optical information processing architectures. As a first demonstration of this method an integrated optical synthetic aperture radar processor is being developed. More general image processing operations are achievable in integrated optics form using the time and space integrating processing method. An architecture is presented that can perform an arbitary linear transformation on an image provided the transformation has a kernel that is separable in the two coordinates. The possibility of photorefractively recording in the waveguide the signals that are necessary to specify the linear transformation using control beams that are external to the plane of the waveguide is explored. Initial experimental demonstration of this idea is reported and an integrated optical vector matrix multiplier that is based on this concept is proposed.

20. DISTRIBUTION/AVAILABILITY OF ABSTRACT: UNCLASSIFIED/UNLIMITED ☐ SAME AS RPT. ☐ DTIC USERS ☐	21. ABSTRACT SECURITY CLASSIFICATION: Unclassified
22a. NAME OF RESPONSIBLE INDIVIDUAL: Col Giles	22b. TELEPHONE NUMBER (Include Area Code): 202 767 4931; 22c. OFFICE SYMBOL: NE

DD FORM 1473, 83 APR EDITION OF 1 JAN 73 IS OBSOLETE.

SECURITY CLASSIFICATION OF THIS PAGE

I Introduction

The goal of this project is the development of techniques that will permit integrated optical devices to be used in inherently nonplanar optical information processing architectures. As a first demonstration of this method an integrated optical synthetic aperture radar (IO SAR) processor is being developed. This is a collaborative effort between Caltech and Professor A. Tanguay's group at the University of Southern California. The basic idea is an extension of the space and time integrating concept that we have previously used to demonstrate bulk acoustooptic processors, including a SAR system[1,2], to an integrated optics implementation. The bulk versions of these systems make use of all three dimensions of the optical system as well as time to perform multidimensional signal processing. Since integrated optics is a planar technology we must find ways to perform spatial integration in the transverse dimension of the IO chip and temporal integration along the direction of propagation. In addition we need methods for communicating information between the guided modes of the IO structure and the free space modes in the third dimension.

In a previous report ("Acoustooptic Synthetic Aperture Radar Processor", Grant AFOSR-84-0319) we have described an architecture for implementing a SAR system in integrated form. This architecture uses distributed holographic coupling out of the integrated plane to address a CCD detector for temporal integration. In this report we describe how this distributed coupling may be implemented using gratings that are holographically recorded in the plane of a lithium niobate waveguide. These gratings can be recorded by interfering a guided mode with a beam incident on the waveguide from the top. Thus we have a method for programming the operation of the IO SAR chip through the third dimension. This method of recording gratings for coupling guided modes to the outside can be naturally extended to implement more general processors. For instance, we can record photorefractive gratings in waveguides which couple guided modes using light incident from outside the waveguide. Based on this method we have designed an integrated optical architecture that is capable of performing an arbitary two dimensional linear transformation with separable kernel (or equivalently a triple matrix product). SAR and 2-D Fourier transforms are two important linear tranformations that can be implemented in this manner. In section II we describe the photorefractive IO architecture. In the following two sections we discuss in detail the two major components of this architecture. We describe in section III a programmable vertical outcoupling mechanism and in section IV an implementation of an integrated vector matrix multiplier that programmable with control beams external to the waveguiding plane.

II Integrated Optical Image Processing Architecture

A separable two dimensional linear transformation takes a function $f(\xi,\eta)$ into a function $g(\xi',\eta')$ according to

$$g(\xi',\eta') = \int_X \int_Y f(\xi,\eta) h_1(\xi,\xi') h_2(\eta,\eta') d\xi d\eta \tag{1}$$

In this architecture one of the two input coordinates (η) is represented by time. Specifically lines of the 2-D image are sequentially entered into the system. We therefore replace the continuous variable η with the integer variable n. The variables ξ and ξ' are represented by the transverse spatial coordinates of the chip at the input and output planes respectively. The output variable η' is represented in the longitudinal, or z, direction of the chip. The above transformation is then written as:

$$g(x',z) = \sum_n \int_X f(x,n) h_1(x,x') h_2(n,z) dx \tag{2}$$

In figure 1 we show the architecture for implementing two dimensional separable linear transformations in integrated optics. The vector f(x,n) is input through a channel waveguide array. Light from each channel is collimated by the lens L_1. The collimated beams are diffracted by a matrix $h_1(x,x')$ of thick gratings associating the input channels with an array of output channels. Each of these gratings specifies a unique interconnection between one channel at the input and one channel at the output. Crosstalk between channels is suppressed by the Bragg condition for volume holograms, $\vec{k}_i - \vec{k}_j = \vec{K}_{ij}$, where $\vec{k}_i$ is the wavevector associated with light collimated form the i^{th} input channel, $\vec{k}_j$ is the wavevector associated with light focused into the j^{th} output channel and $\vec{K}_{ij}$ is the spatial frequency of the sinusiodal hologram connecting channel i to channel j. In the case of integrated interconnections, all of the beams of interest are confined to a single plane. In this plane the two wavevectors satifying the Bragg condition for a grating at spatial frequency K are unique. This is shown graphically in figure two for a 3×3 interconnection scheme.

The lens L_2 focuses the diffracted input light into the output channels. The light in these channels is holographically coupled out of the plane onto a CCD. In the case shown in figure 1 the coupling efficiency between the channels and the CCD is modulated along the length of the waveguides using a 1-D series of electrodes addressed at the sampling frequency to electrooptically modulate the spatial frequencies of the guided modes and thus control the Bragg matching between these modes and the radiation modes incident on the CCD. In this way the light detected at each pixel on the CCD is modulated by

$h_2(n,z)$, where z is a spatial coordinate along the length of the waveguides. h(n,z) might also be implemented by placing a dynamic spatial light modulator between the waveguides and the CCD. After N pulses the charge distribution that accumulates on the CCD is proportional to

$$g(x',z) = \sum_n \int_X f(x,n)h_1(x,x')h_2(n,z)dx \tag{3}$$

Thus our architecture implements exactly transformations of the sort described in equation 2.

The gratings that are necessary for outcoupling light from the waveguide to the CCD can be recorded holographically using the photorefractive effect. This is described in the following section. The gratings that are needed to specify the linear transformation at the front end of the processor are also recorded holographically by interfering in the photorefractive waveguide beams incident from above. The details of how this is done are described in the fourth section.

III Channel to CCD Coupling

In this section we consider vertical outcoupling from waveguides for out of plane processing. In particular, we describe how vertical outcoupling might be implemented in the IO SAR architecture described in our previous report. The IO SAR architecture is completely analogous to the more general linear transformation architecture except for the fact that in the IO SAR case the mask between the waveguide and the CCD need not be dynamic on the time scale of the pulse repetion frequency. In architectures for which dynamic masks are required, the electrooptic scheme described in the previous section might be employed.

Synthetic aperture radar is an imaging radar system which uses the relative motion of the radar and target to obtain crossrange information from doppler shifts in the returning radar pulses. Range is recovered in the IO SAR processor by spatial integration of returned pulses introduced to the device through acoustic transducers. This part of the device is described in our earlier report.

Azimuth is recovered in the IO SAR processor by a temporally integrated correlation of the range focused signal against a reference kernel stored in a two dimensional mask covering a channel array to CCD interface. This mask modulates the field coupled from the channels to the CCD by

$$T(x,z) = \frac{1}{2}(1 + cos(\frac{b_2 z^2}{x})) \tag{4}$$

where b_2 is a constant. Note that we have not included in this equation the carriers necessary to separate the full complex image from the bias terms. The system as described here allows the recovery of only the real part of the image. The carrier encoding mechanisms are described in detail in references [1] and [2] for the bulk architecture. The same methods apply to the integrated system. Since in the IO SAR processor the light in each channel must be sampled many times along the z direction, T(x,z) must be implemented such that the channels are only slightly perturbed at any given location. In this section we describe how T(x,z) may be implemented using holographic and photolithographic techniques to modulate the amplitude of perturbations in the refractive index of the waveguiding plane.

Grating couplers are commonly used in integrated optics to boost spatial frequencies associated with radiation modes to guided frequencies[3]. A prototype geometry for these devices is shown in figure 3. The grating consists of a periodic perturbation to the effective permitivity of the waveguide. The perturbation may be implemented by etching physical rulings as in figure 3 or by changing the actual index of the waveguiding film. One method of fabricating gratings uses standard etching methods to record interference

patterns created by two beam mixing in light sensitive films. Grating couplers have been made in photoresist by this method at USC as part of this project.

The modulation T(x,y) could be applied directly to a grating coupler by using photolithographic masks or optical elements to modulate one or both of the writing beams during grating formation. Since the the frequency and chirp rate of T(x,y) depend on potentially variable aspects of the radar system geometry, the utility of the IO SAR processor would be greatly extended if it were possible to write the grating coupler in real time. In light of this fact and in light of the long established use of $LiNbO_3$ in holographic applications, we consider photorefractive holography directly in the waveguide array to be a most promising means of vertical outcoupling for the IO SAR and other image processing architectures.

The photorefractive effect is a process by which a spatial refractive index may be written in electro-optic crystals by spatially inhomogeneous optical fields[9]. The basic mechanism may be visualized by considering figure 4. Two coherent light beams with wavevectors $\vec{k}_1$ and $\vec{k}_2$ create a fringe pattern of frequency $(\vec{k}_1 - \vec{k}_2)$ in their region of intersection. Charge carriers are excited from local trap sites in the photorefractive crystal. These carriers migrate to low intensity regions, where they are trapped again. This migration may be driven by an external field, by diffusive relaxation of the inhomogeneous carrier density, or by inhomogeneity in the $\vec{k}$ vector distribution of the excited carriers. In $LiNbO_3$ this last mechanism, the anomalous bulk photovoltaic effect[4], is dominant in most applications. The migration of charge carriers from regions of high intensity to darker regions establishes a space charge field. The space charge field in turn modulates the refractive index of the crystal via the electro-optic effect, thus establishing in the crystal a phase grating of period $\frac{2\pi}{(\vec{k}_1 - \vec{k}_2)}$.

The dielectric permitivity perturbation established in a photorefractive thin film waveguide by two radiation modes may be modeled to a first approximation as

$$\Delta\epsilon = h(x,y)cos(kz + \phi)$$

where $k = (\vec{k}_1 - \vec{k}_2)_z$. This perturbation leads to the exchange of energy between modes at frequencies β_ν and $\beta_{\nu'}$ where $\beta_\nu \quad \beta_{\nu'} = +k$

The coupling between mode ν and mode ν' may be described in the adiabatic approximation by the coupled equations

$$\frac{dA_\nu}{dz} \quad j\kappa_{\nu\nu'}A_{\nu'}$$

$$\frac{dA_{\nu'}}{dz} \quad j\kappa_{\nu'\nu}A_\nu$$

where

$$\kappa_{\nu\nu'} = \frac{\mu\omega^2}{2\beta_{\nu'}} \int\int h(x,y)\vec{\mathcal{E}}_{\nu}(x,y) \times \mathcal{H}_{\nu'} dxdy$$

$\mathcal{E}$ and $\mathcal{H}$ are the normalized electric and magnetic field distributions of the modes and A_ν is the amplitude of the ν^{th} mode. Typically the coupled modes will be the fundamental guided mode and the Bragg matched radiation mode. In the case of the IO SAR processor we are not concerned with the exact radiation mode into which the guided light is coupled since the CCD is close enough to the waveguide array that all free space radiation modes will be detected. It is important of course that the separation be large enough that the high dielectric constant of the silicon CCD does not perturb the waveguide.

In the geometry we are proposing the modulation T(x,z) is written on the much higher frequency carrier $\cos(kz + \phi)$. Since the outcoupling is driven at the higher frequency, the distributed nature of the coupling may be ignored so long as

$$\frac{T'(x,z)}{T(x,z)} \ll k$$

where $T'(x,z) = \frac{\delta T}{\delta x}$. In this case the only adjustment that need be made to the kernel T(x,z) on account of its longitudinal implementation is that the amplitude of the perturbartion must increase along the guide to account for the decay of the guided mode.

While a number of experiments have been performed using the photorefractive effect in $LiNbO_3$ indiffused waveguides to write holograms transverse to the propagation direction[5,6,7], writing a grating along the optical axis provides new challanges. In all experiments published to date the write beams have been guided. It is not feasible to use guided write beams for our purposes because it is difficult to form gratings along the optical axis with guided beams and because using guided write beams in a multi-element geometry would be damaging to the properties of system outside of the mask region. For these reasons and for the advantages in framing grating parameters offered by the extra degrees of freedom avaliable to radiation modes, we propose to use these modes to write the grating for vertical outcoupling in the IO SAR processor.

Longitudinal gratings are more difficult than transverse gratings to implement in $LiNbO_3$ waveguides for materials reasons. The key mechanism driving excited carrier migration in $LiNbO_3$ is the bulk photovoltaic effect. The principal direction of charge migration under this effect is along the c axis. For gratings written along this axis the applicable electro-optic coefficients are r_{13} and r_{33}. r_{33} is about three times r_{13}. If the read mode for the grating propagates transverse to z the r_{33} coefficient may be read by a mode with the extraordinary polarization. If the read mode is longitudinal then the extraordinary index is not available and the r_{13} coefficient must be used. This is problematic both because $r_{13} < r_{33}$ and because it is not desirable for the guided mode to use the ordinary polarization for reasons to be described below. One way in which

these difficulties may be addressed is by writing the grating along 100 and using the r_{51} coefficient, but in this case the grating must be written by carrier diffusion which results in low sensitivity. Another possibility is to search for crystal geometries away from the crystalographic axes that may offer acceptable compromises.

Photorefractive holography offers a flexible if challenging means of developing vertical outcoupling for two dimensional processing. While it is difficult to find geometries that maximize both the holographic sensitivity and the waveguiding characteristics of the crystal, it does appear the geometries may be found in which a satisfactory compromise is available.

IV Photorefractive Integrated Optical Vector Matrix Multiplier

In this section we describe how out of plane photorefractive holography may be used to control coupling between in plane guided modes and in particular how photorefractive holography may be used to implement an integrated vector matrix multiplier. As discussed in the previous section, photorefractive gratings arise from the electro-optical modulation of the refractive index by the space charge field arising from the inhomogeneous charge distribution induced by the intensity distribution of the write beams. A particular geometry for applying this effect in the integrated setting uses the radiation modes $E_{r1}(\vec{r}) = A_{r1}\mathcal{E}_{r1}(x)e^{j\vec{\beta}_{r1}\cdot\vec{r}}$ and $E_{r2}(\vec{r}) = A_{r2}\mathcal{E}_{r2}(x)e^{j\vec{\beta}_{r2}\cdot\vec{r}}$ to modulate the dielectric susceptibility of the waveguiding substrate according to[9]

$$\Delta\chi = -\varepsilon r\vec{E}_{sc}\varepsilon$$

where ε is permittivity tensor and r is the linear electro-optic tensor. The space charge field is given by

$$\vec{E}_{sc} = E_{eff}M_{12}\vec{\beta}_{12}cos(\vec{\beta}_{12}\cdot\vec{r}+\phi)$$

Where M_{12} is the modulation depth of the intensity induced charge distribution and $\vec{\beta}_{12} = \vec{\beta}_1 - \vec{\beta}_2$. We have assumed that $M_{12} \ll 1$. The magnitude of E_{eff} depends on the dominant photocharge migration mechanism. The three possible candiates are drift in an applied field, diffusion and the bulk photovoltaic effect. In the drift case the space charge field is not linear in the grating wavevector.

The phase grating induced by the radiation modes couples the guided modes at spatial frequencies $\vec{\beta}_{g1}$ and $\vec{\beta}_{g2}$ such that $\vec{\beta}_{g1} - \vec{\beta}_{g2} = \vec{\beta}_{12t}$ where $\vec{\beta}_{12t}$ is the component of $\vec{\beta}_{12}$ which lies in the plane of the waveguide. The component out of the plane must satisfy $\beta_{12x}d \ll 1$ where d is the effective thickness of the waveguide. Taking the field distributions of the coupled modes to be $E_1(\vec{r}) = A_1(y)\mathcal{E}_1(x)e^{j(\vec{\beta}_1\cdot\vec{r}-\omega t)} + c.c.$ and $E_2(\vec{r}) = A_2(y)\mathcal{E}_2(x)e^{j(\vec{\beta}_2\cdot\vec{r}-\omega t)} + c.c.$ the coupled wave equations for A_1 and A_2 in the slowly varying envelope approximation are

$$\frac{dA_1}{dy} = -j\frac{k_o^2}{2\beta_1}E_{eff}M_{12}\langle\varepsilon r\vec{\beta}_{12}\varepsilon\rangle e^{j(\Delta y+\phi)}A_2\int_{-\infty}^{0}\mathcal{E}_1^*(x)\mathcal{E}_2(x)e^{j\beta_{12x}x}dx$$

$$\frac{dA_2}{dy} = j\frac{k_o^2}{2\beta_2}E_{eff}M_{12}\langle\varepsilon r\vec{\beta}_{12}\varepsilon\rangle e^{-j(\Delta y+\phi)}A_1\int_{-\infty}^{0}\mathcal{E}_2^*(x)\mathcal{E}_1(x)e^{-j\beta_{12x}x}dx$$

Where $\Delta = \beta_{12y} - (\beta_{1y} - \beta_{2y})$. We have assumed that the modulation depth is not x dependent. If we also assume that the anisotropy of the waveguide is small and that $\beta_{12x}d \ll 1$ then for well guided modes

$$\int_{-\infty}^{0}\mathcal{E}_2^*(x)\mathcal{E}_1(x)e^{-j\beta_{12x}x}dx = \delta_{\nu_1\nu_2}$$

where ν_i is the order of the respective guided mode. The condition that the modes be well guided allows us to ignore the field outside of the substrate. If $\nu_1 = \nu_2$, the coupling efficiency will be large if $\Delta \ll \frac{k_0^2}{2\beta_2} E_{eff} M_{12} \langle \varepsilon r \vec{\beta}_{12} \varepsilon \rangle$

In the case of vector matrix multiplication, $n_1 n_2$ gratings are used to map n_1 input frequencies to n_2 output frequencies. Each grating is associated with a pair of radiation modes using the rotational degeneracy of the write and read beams about the grating vector. Consider the rotation α which takes the input component $\vec{k}_1$ into the radiation mode with wavevector $\vec{K}$ by rotation about $(\vec{k}_1 - \vec{k}_2)$. The equations $\alpha \vec{k}_1 = \vec{K}$ and $\alpha(\vec{k}_1 - \vec{k}_2) = (\vec{k}_1 - \vec{k}_2)$ may be solved simultaneously if and only if $(\vec{K} - \vec{k}_1) \cdot (\vec{k}_1 - \vec{k}_2) = 0$. This equation in concert with the constraints $\vec{k}_2 \cdot \hat{e}_x = 0$ and $|k| = k_0$ specify $\vec{k}_2$ to one of at most two vectors. This is shown graphically in figure 5. Any two vectors with end points on the arcs on the normal surface separated by $(\vec{k}_1 - \vec{k}_2)$ which form a plane normal to the arcs may be used to read or to write the grating with frequency $(\vec{k}_1 - \vec{k}_2)$. However, there need not exist a single $\vec{K}$ out of the plane of $\vec{k}_1, \vec{k}_2, \vec{k}_3$ such that $\vec{K}$ may be used to write both grating vectors shown in figure 5. Thus it is not possible to represent $\vec{k}_1$ by a single radiation mode for all n_2 gratings associated with it. In general as many as $2n_1 n_2$ points in Fourier space must be available in the radiation modes to write all $n_1 n_2$ gratings. One means of presenting all these modes simultaneously might be to use a second volume hologram to store the $2n_1 n_2$ beams. Since the intensities of all these beams should lie on the same range, the modulation depth of each grating writen by this approach will be proportional to $(n_1 n_2)^{-1}$. The modulation depths of the individual gratings are also proportional to $(n_1 n_2)^{-1}$ for sequential writing if the asymmetry between the erase and write times is not large. It is possible to reduce this reduction factor to $(\sqrt{n_1 n_2})^{-1}$ by writing all the grating with a single reference beam. A large modulation depth is desirable since the diffraction efficiency of a hologram is proportional to the square of the modulation depth.

The architecture shown in figure 6 allows for a simple writing geometry with a single reference by relaxing the constraint of exact phase matching. A vector is input through a channel waveguide array integrated on a suitable substrate. Light from these channels is collimated by integrated lenses[10] before reading out a matrix of holograms formed in a slab waveguiding region. The diffracted vector is refocused into an output channel waveguide array. Each spatial frequency in the grating matrix connecting the input channel waveguide array with the output array is addressed from above the integrated plane by a single pixel in the input mask T. Light collimated from these pixels interferes with the reference plane wave R to create the desired gratings. The lenslet array LA may be added to focus light from an extended beam onto the mask T in order to increase efficiency. The modulation depth of the $(ij)^{th}$ grating is

$$M_{ij} = \frac{\sqrt{I_{ij} I_R}}{I_R + N\langle I_{ij} \rangle}$$

Where I_{ij} and I_R are the intensities of the $(ij)^{th}$ write beam and of the reference

respectively. $\langle I_{ij} \rangle$ is the mean value of the write beam intensities. The expected value of M_{ij} has a maxima of $(2\sqrt{(n_1 n_2)})^{-1}$ when $\langle I_{ij} \rangle = \frac{I_B}{\sqrt{(n_1 n_2)}}$. The Fourier lens L_1 is aligned so that a pixel on its optical axis is collimated such that

$$\kappa_{00_x} = K_x;\ \kappa_{00_y} = K_y = 0;\ \kappa_{00_x} = -K_z$$

where $\vec{\kappa}_{00}$ and $\vec{K}$ are the wavevectors of the collimated beam and of the reference respectively. The requirement that the grating produced by the reference and the light from pixel ij form the grating between the i^{th} input channel and the j^{th} output may be expressed $\vec{\kappa}_{ij} = \vec{K} - \vec{k}_{ij}$. Since $\vec{k}_{ij}$ has no component out of the plane of the waveguide, the $\hat{e}_x$ component of this equation is satisfied if, as we saw above,

$$(\vec{K} - \vec{\kappa}_{ij})_x \ll \frac{1}{d}$$

In the paraxial approximation this requirement becomes $\frac{\rho}{F} \ll \sqrt{\frac{\lambda}{d}}$ where ρ is the radius of T. Having satisfied this constraint, the $\hat{e}_y$ and $\hat{e}_z$ components of the phase matching equation may be satisfied by properly placing the pixels in the Fourier plane. An example of a suitable mask for a four by four device with a 400 μm separation between channels is shown in figure 7. We have assumed F=25 cm, $f_1 = f_2 = 1$ cm. The angle between the writing beams is assumed to be three degrees.

We have written photorefractive gratings in single mode titanium indiffused slab waveguides on nominally pure y cut $LiNbO_3$. The gratings were written using unguided light at 488 nm from an Ar^+ laser. The red HeNe line was used for readout. The grating wave vectors were nearly parallel to the c axis to make use of the r_{33} electrooptic coefficient and the photovoltaic field. Optical propagation was along 010 for the write beams and along 100 for the guided read beams. The effective index for the guided HeNe mode was 2.248, while the extraordinary index of the substrate at 488 nm is about 2.6. Thus, between the write and read beams there was an expansion of the angle between the beams Bragg matched to a particular grating by a factor of about 1.5. Small angles were used because our waveguide was not guiding along c. We have obtained coupling efficiencies of up to 4.5% between guided modes of interaction lengths of about 1 cm. We have also been sucessful at coupling a single guided mode into two two diffracted modes, though we have not yet implemented the mask scheme described above to achieve multibeam coupling with high efficiency. Photographs of zero and first order spots diffracted from the end of the waveguide in the one and two grating cases are shown in figure 8.

Various problems arise in the implementation of the architecture we have proposed. Two specific problems concern the depletion of the pump beams and the implementation of the matrix in grating amplitudes. Since the interaction region for integrated volume holograms may be very long, the coupling efficiency of these holograms may be quite high. In the depleted pumps regime the accuracy to which the device represents a true

vector matrix multiplier will be compromised. The extent to which this is a problem depends upon the application envisioned. Since the amplitude of each grating is linear in modulation depth, which is a nonlinear function of the total background intensity, it is only possible in a statistical sense to associate a given grating amplitude with a specific transmittance in the writing mask. For small scale applications both of these problems may be surmounted by considering the expected signals from each channel. For larger scale applications, the application must be tolerant to these nonlinearities. Optical neural computers[11] are one such application, but it seems unlikely that the device described here could be implemented on a scale which would be useful in neural computation.

A third problem arises from the effect of titanium on the photorefractive properties of $LiNbO_3$. Glass *et. al.* found that Ti doping increases the dark conductivity of $LiNbO_3$, thereby reducing the grating storage time[8]. In our waveguides we found grating lifetimes of several days under continuous guided readout with about 50 μW. One method of increasing this lifetime might be to use proton exchanged waveguides[12]. In applications where storage time is not a concern, GaAs or SBN might be used as a substrate.

V References

[1] D. Psaltis and K. Wagner, *Opt. Eng.* **21**,822(1982).

[2] D. Psaltis, M. Haney, and K. Wagner, Proc. *NASA Conference on Optical Information Processing for Aerospace Applications II*, Langley, Virginia, 1983.

[3] See for example T. Tamir, in *Integrated Optics*, T. Tamir ed, Berlin: Springer-Verlag, 1979.

[4] A.M. Glass, D. von der Linde, and T.J. Negran, *Appl. Phys. Lett.* **25**,233,(1974).

[5] R.P. Kenan, D.W. Vahey, N.F. Hartman, V.E. Wood, C.M. Verber, *Opt.Eng.* **15**,12(1976).

[6] O.V. Kandidova, V.V. Lemanov, B.V. Sukharev, *Sov.Phys. Tech. Phys.* **29**,1019(1984).

[7] W.S. Goruk, P.J. Vella, R. Normandin, G.I. Stegeman, *Appl. Opt.* **20**,4024(1981).

[8] A.M. Glass, I.P. Kaminow, A.A. Ballman, D.H. Olson, *Appl. Opt.* **19**,276(1980).

[9] N.V. Kukhtarev, V.B. Markov, S.G. Odulov, M.S. Soskin V.L. Vinetskii, *Ferroelectrics* **22**,949(1979).

[10] D.Y. Zang, C.S. Tsai, *Appl. Opt.* **25**,2264,(1986).

[11] D. Psaltis and N. Farhat, *Opt. Lett.* **10**,98(1985).

[12] J.L. Jackel, C.E. Rice, J.J. Veselka, *Appl. Phys. Lett.* **41**,607(1982).

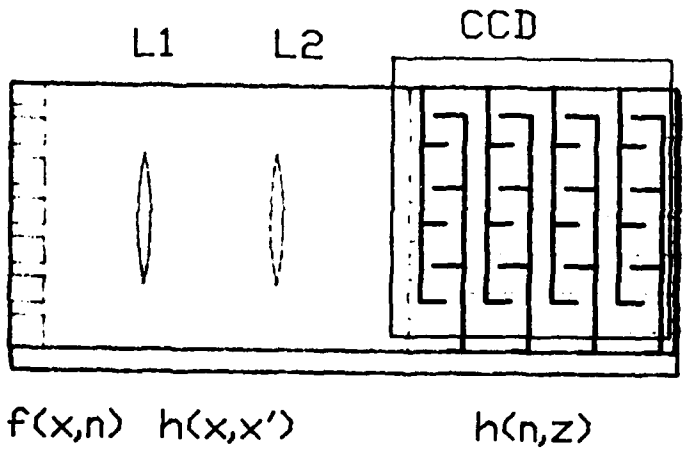

Figure 1. A general integrated triple matrix processor architecture.

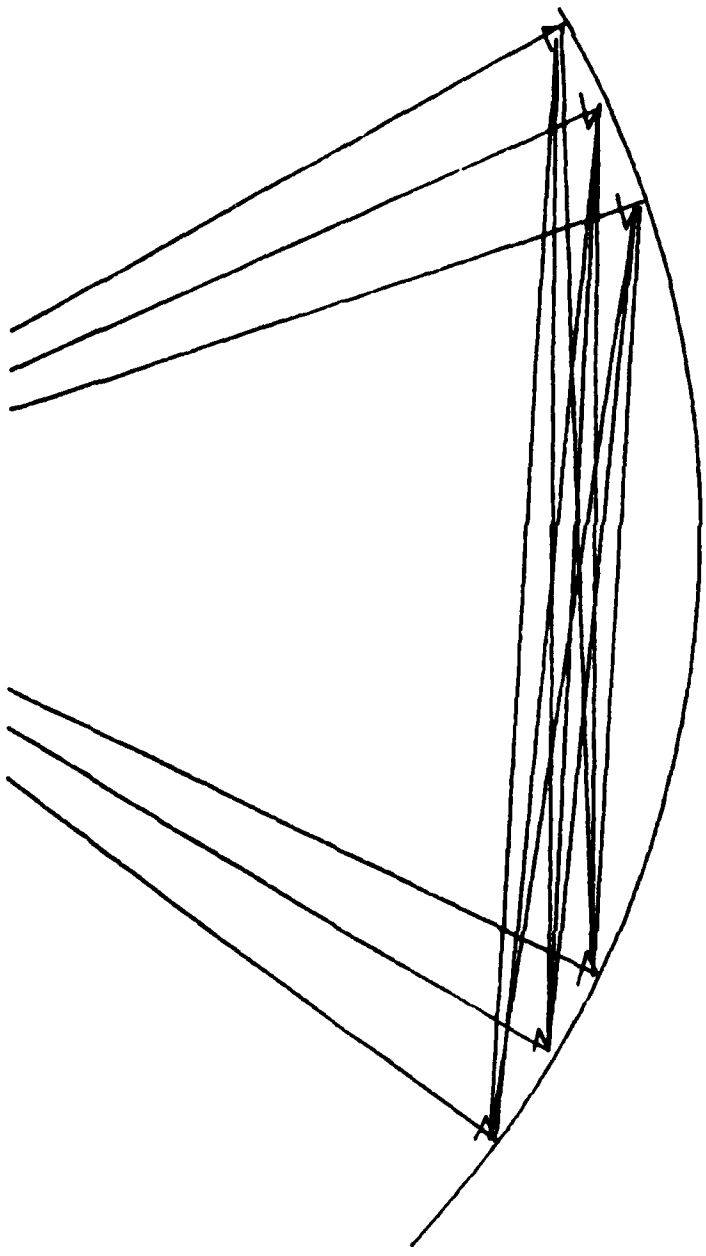

Figure 2. A phase space diagram of a 3 × 3 interconection matrix

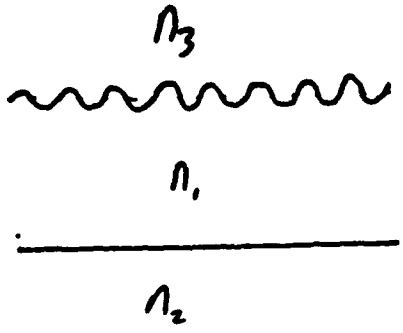

Figure 3. Grating coupler geometry.

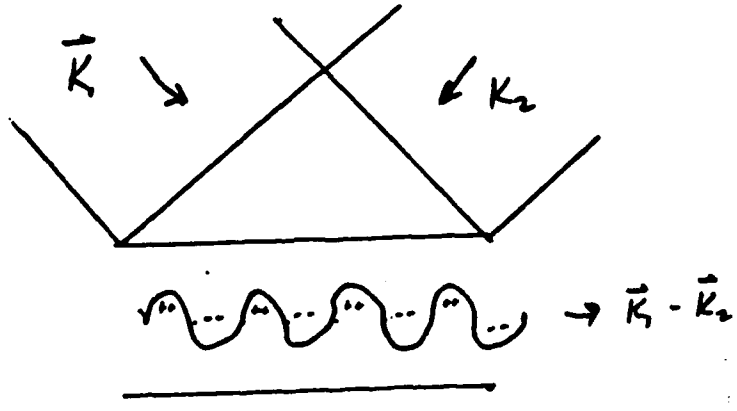

Figure 4. Photorefractive grating formation.

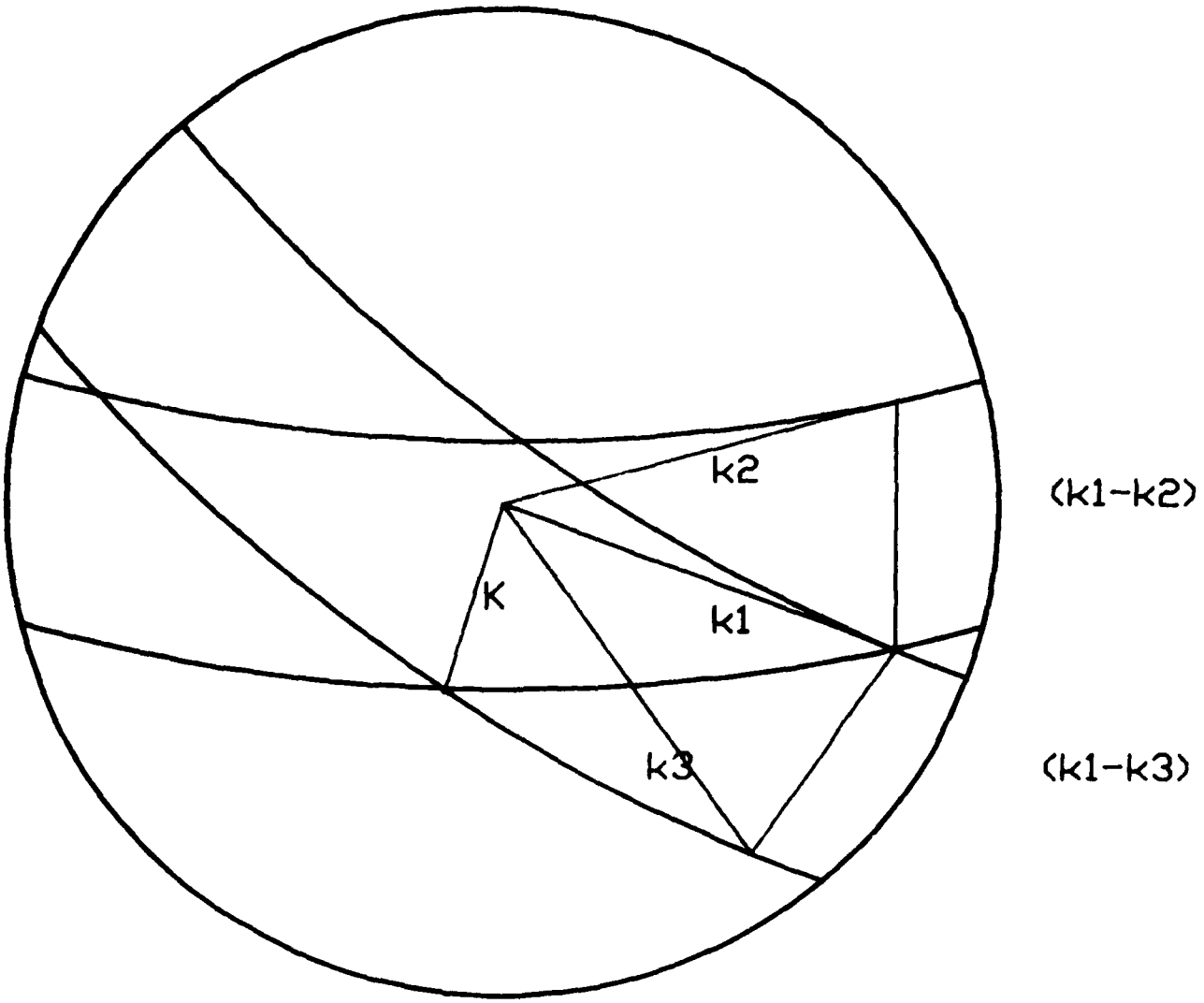

Figure 5. Out of plane rotational degeneracy.

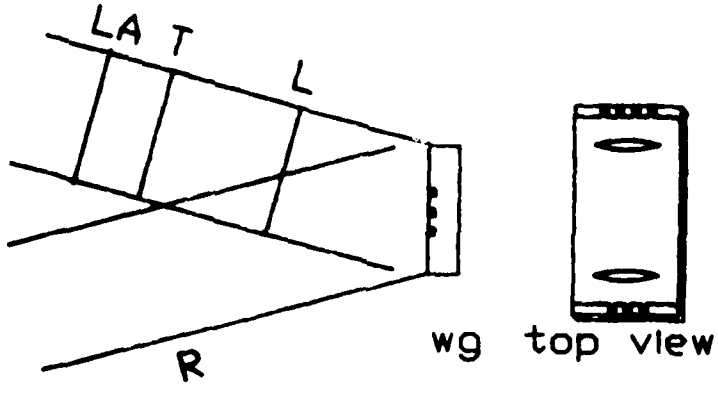

Figure 6. Vector matrix multiplier geometry.

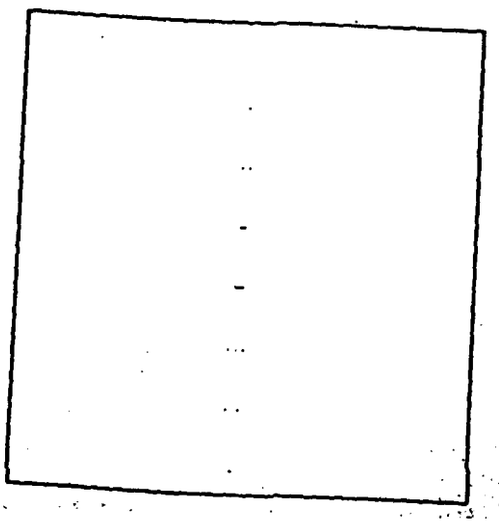

Figure 7. Recording mask for 4 × 4 matrix.

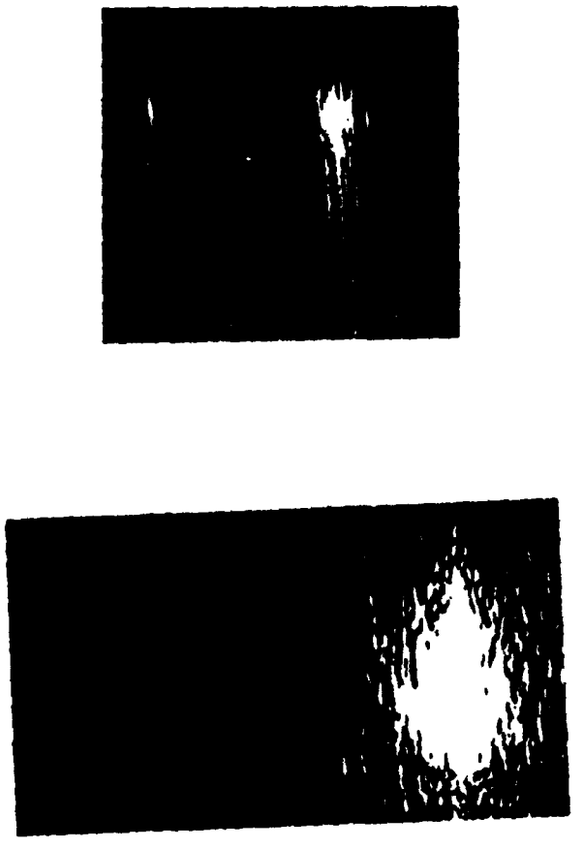

Figure 8. Spots scattered from the end of a waveguide containing one and two gratings written from out of the plane. Diffracted spots are on the left.

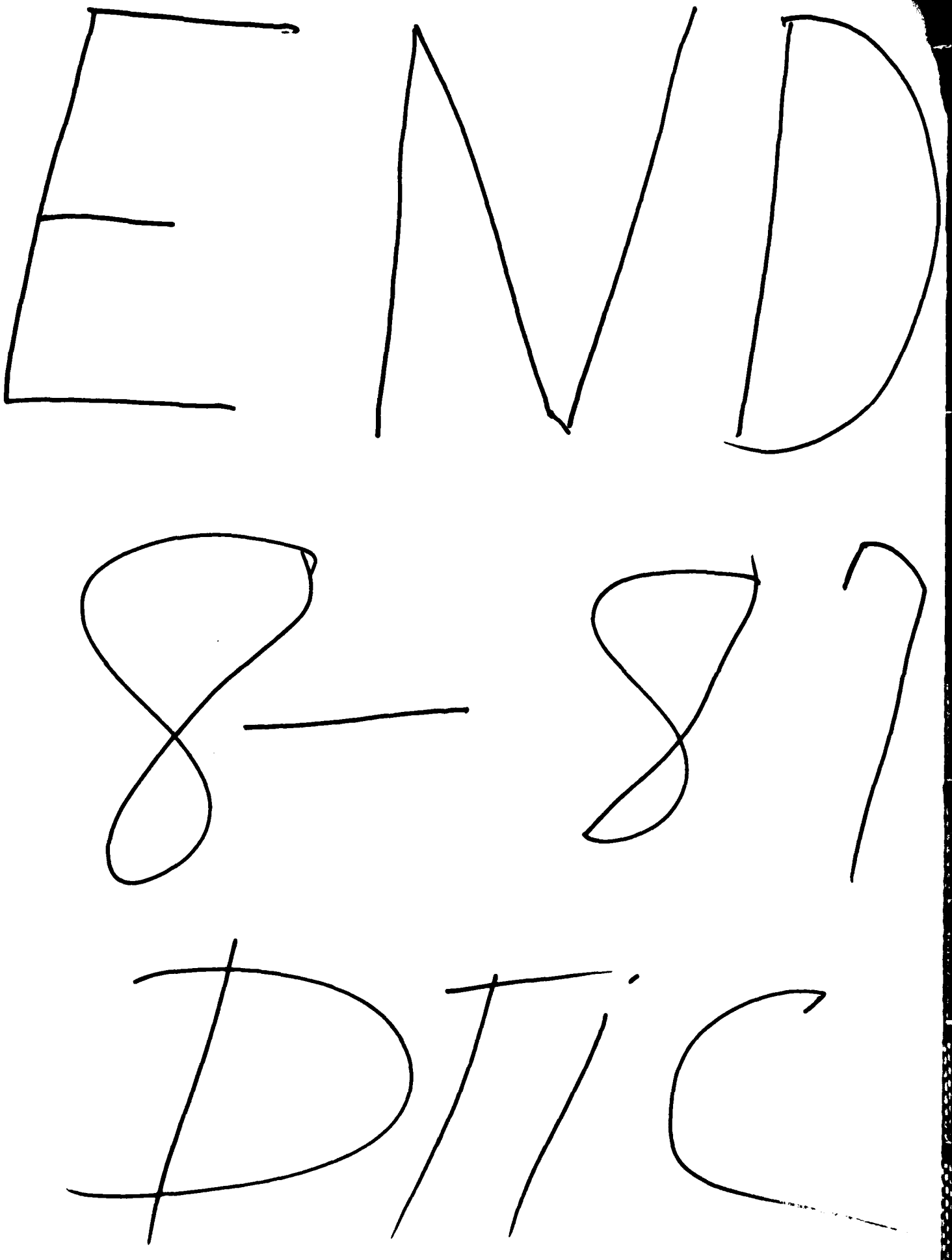
END
8-87
DTIC